A dynamic configurable sensor for fractional-octave-band underwater acoustic measurements

Legg M.W. (1) and Matthews, D.N. (1,2)

(1) MOD, Defence Science and Technology Organisation, HMAS Stirling, Western Australia
(2) CMST, Curtin University of Technology, Bentley, Western Australia

ABSTRACT

This paper reports on an underwater acoustic sensor used to demonstrate dynamic configurable Field Programmable Analogue Array (FPAA) devices. A single FPAA device was connected to a microcontroller and programmed to sweep through a set of fractional one-third octave filters with centre frequencies from 100 Hz through 20 kHz. Fourth order filters were designed using a cascading topology and approximated using two second order filters available in the FPAA. Sweep timing characteristics were controlled by the microcontroller to allow for settling time and a predetermined estimation uncertainty for each fractional octave band. Laboratory testing compared the filters with the relevant ANSI standard. Field measurements were conducted in the shallow waters of Cockburn Sound. Results of laboratory and field measurements are presented and discussed.

INTRODUCTION

Sensors and devices that allow dynamic configuration can be used to enable or enhance underwater measurement systems, particularly when data reduction at the sensor level is desired (Lavoie & Pollard 2001) or in modular systems where a fixed suite of hardware must be configured to perform different tasks (Koay et al. 2010).

Consider the problem of recording underwater ambient noise from a small, deployable device (Simão et al. 2010) or a device fitted to an underwater vehicle with limited space and power availability (Eriksen et al. 2001). Sampling the ambient noise as a time-series may not be possible if high sample rates or long observation times are desired. Under such circumstances it may be acceptable to reduce the data through signal processing; for example sampling the average RMS power every few seconds instead of the full time-series. In recent times the trend has been toward implementing digital solutions for such signal processing tasks, however, low-power analogue options are possible (Hall et al. 2005).

Field Programmable Analogue Array (FPAA) devices provide an analogue alternative to digital signal processing for a set of rudimentary signal processing tasks. An advantage of FPAA devices is that the signal remains analogue, eliminating the need for repeated analogue-to-digital followed by digital-to-analogue conversions when retention of an analogue signal is required. This in turn reduces the number of devices required to achieve the signal processing task and can reduce the space and (for continuous time FPAAs) power requirements when a signal path having both analogue input and analogue output is desired. Some examples where FPAA devices have application include electrocardiogram signal analysis (Morales et al. 2010), sensor signal conditioning (Merendino et al. 2005, Baccigalupi & Liccardo 2007), sensor auto-calibration (Koudier et al. 2003) and enhancing the resolution of analogue-to-digital converters (Morales et al. 2008). Switched capacitor FPAA devices are subject to some well-known disadvantages including clock noise and aliasing, and they use more power than continuous-time (non-switching) FPAA devices but they have the advantage of being more flexible (Becker et al. 2008).

With these advantages and disadvantages in mind, this study investigates the ability of a single FPAA device to achieve a moderately difficult signal processing task: to iteratively sweep through a bank of one-third octave filters.

One-third octave filters belong to the general family of fractional-octave filters defined using either the ANSI or ISO standard. Fractional-octave filters are characterised by a constant relationship between the bandwidth of the filter and the centre frequency of the filter or alternatively by the Q of the filter. For this reason fractional-octave filters are also referred to as constant-Q filters (Smith 2008). A bank of fractional-octave filters commonly encountered in audio signal processing are the constant-Q graphic equalisers, a testament to the origins of one-third octave processing being associated with human hearing (Dahl et al. 2007, Smith 2008). Many acoustic and vibration measurement devices, such as sound level meters, make use of fractional-octave filter banks because they are well suited to spectral analysis of broadband signals (ANSI S1.11-1986). Fractional-octave band analysis is of general interest to scientists and engineers in acoustics and vibration (Bjor 2008) and provides a method of data reduction useful for analysis and comparison of underwater sounds (Matthews, MacLeod & McCauley 2004, Dahl et al. 2007).

This paper introduces the problem of underwater measurement using space and resource limited systems and discusses the FPAA device applied to that problem. A moderately difficult signal processing task is proposed to further investigate the capability of a single FPAA device. The methods used to design one-third octave filters are given followed by noise and aliasing issues internal to the FPAA device. The use of a microcontroller is introduced for programming and controlling the FPAA and methods for sweep timing, exposure and post-processing are outlined. Laboratory testing results are presented and compared with the ANSI standard. Field trial results are presented followed by a discussion of sensor performance and some concluding remarks.

Field Programmable Analogue Arrays

Field Programmable Analogue Arrays are a family of devices containing analogue components and component blocks that can be joined together in a number of different configurations using digitally controlled switching. FPAAs are grouped into two sub-types: continuous-time (CT) and switched-capacitor (SC) (Becker et al. 2008). Continuous-time FPAAs provide improved bandwidth and lower power consumption whereas switched-capacitor FPAAs are more flexible. Attention is restricted to the switched-capacitor (SC) sub-type for the purpose of this sensor.

The analogue systems in a switched-capacitor FPAA are organised into functional groups that can be loosely categorised as either an Input-Output Cell (IOCell) or a Configurable Analogue Block (CAB). IOCells control how the device interfaces with an external input or output and may include some amplification or active filter functionality. CABs provide the basic building blocks for analogue signal processing based on conventional and switched capacitor op-amp circuits (Anadigm 2008). The functionality of a CAB can be modified by changing the connection of components within the functional group, for example the gain of a CAB configured as an amplifier can be adjusted by choosing different ratios of switching capacitors from a capacitor bank. To obtain a full signal processing chain an input IOCell connects to one or more CABs configured to give the desired signal processing and the output connected to another IOCell.

An Anadigm AN231E04 FPAA device was used for the demonstration sensor. The device provided seven IOCells and four CABs for analogue functionality, and support functions including voltage references, a lookup table and a digital SPI configuration interface. Bundled with the development board for the device was a software package called AnadigmDesigner2. The AnadigmDesigner2 software was used to visually design the FPAA functionality (a one-third octave filter) and output C code for programming the design into a microcontroller.

METHOD

Fractional one-third octave filter design

Of the four CAB processing blocks available in the FPAA one was required for a frequency variable anti-alias filter and one was required for gain correction; leaving two blocks for the one-third octave filter(s). A single CAB can be configured as a second order bi-quadratic filter so the two available CABs could be used in cascade to create a fourth-order filter, as shown in Figure 1. The generic filter parameters were designed using the cascading topology described by Kugelstadt (2002). It will be shown that the *design order* of the filter (related to the mathematical design as given in Kugelstadt (2002)) resulted in a realised filter with only half the *ANSI order* when compared with the ANSI standard. To distinguish, the term *order* has been assigned to the design order with any specific reference to the ANSI order using the term *ANSI-order*.

The transfer function $H(s)$ of a fourth order filter designed as a cascade of two second order filters is given in Equation 1 (Kugelstadt 2002) with A_{mx} the gain at the mid-frequency of each sub-filter, Q_x the Q-factor of each sub-filter and α a factor by which the mid-frequency of each sub-filter differs from the centre frequency. The subscript x in A_{mx} and Q_x refers to either of the two sub-filters.

$$H(s)=\left[\frac{\alpha s\left(\frac{A_{m1}}{Q_1}\right)}{1+\frac{\alpha s}{Q_1}+(\alpha s)^2}\right]\left[\frac{\left(\frac{s}{\alpha}\right)\left(\frac{A_{m2}}{Q_2}\right)}{1+\frac{s}{\alpha Q_2}+\left(\frac{s}{\alpha}\right)^2}\right] \quad (1)$$

Parameter α can be computed by numerically solving Equation 2 with specific parameter values. For this task the MATLAB *solve* routine was used. The *solve* routine is part of the symbolic math toolbox and is based on a MuPAD symbolic math engine (see http://en.wikipedia.org/wiki/MuPAD).

$$\alpha^2+\left[\frac{\alpha(\Delta\Omega)a_1}{b_1(1+\alpha^2)}\right]^2+\frac{1}{\alpha^2}-\frac{(\Delta\Omega)^2}{b_1}-2=0 \quad (2)$$

Specific parameters for a one-third octave implementation are given in Table 1. The table includes an overall filter design Q and a corrected value Q_d that accounts for the order of the filter as specified in the ANSI standard. For the fourth order design outlined here, the correction is for an ANSI-order two filter.

Table 1. Design parameters for a one-third octave filter with corrections for an ANSI-order two filter.

a_1	1.414
b_1	1.000
Q	4.318
Q_d	4.796
$\Delta\Omega$	0.2085

Numerical solution of Equation 2 using the *solve* routine provided many possible solutions of which α=1.077 compared well with tabulated results in (Kugelstadt 2002). Sub-filter parameters using α=1.077 are shown in Table 2.

Table 2. Sub-filter parameters for a fourth order one-third octave filter given α=1.077

$A_{m1}=A_{m2}$	1.418
$Q_1=Q_2$	6.801

For a given one-third octave filter with centre frequency f_c each sub-filter was designed using the parameters given in Table 2 and sub-filter centre frequency f_{cx} as shown in Equations 3.

$$f_{c1}=\frac{f_c}{\alpha} \qquad f_{c2}=f_c\alpha \quad (3)$$

The filter bank produced for this paper was a monotonic increasing set of one-third octave filters with centre frequencies from 100 Hz to 20 kHz, defined as the ANSI bands 20 through 43. The ANSI standard (ANSI S1.11-1986) allows two methods for computing the mid-band frequency for each filter; one is a base 10 method, and the other a base 2 method. The base 2 method is intended for use in clocked systems allowing the underlying filter construction to remain unchanged while doubling the clock frequency to give filters for successive octaves. However, the intention was to investigate the effects of adjusting the underlying filter construction and for this reason the base 10 method was chosen.

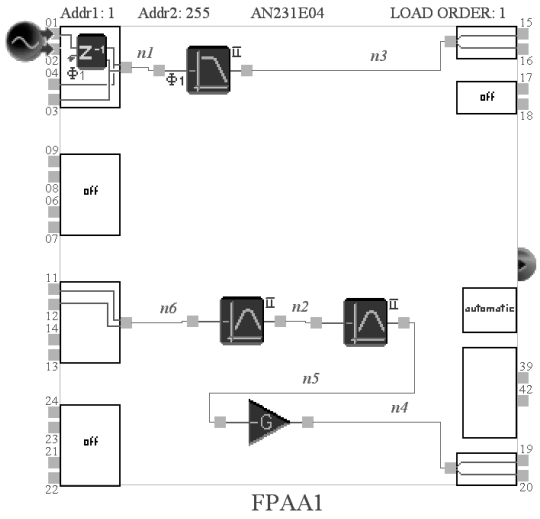

Figure 1. Sensor filtering designed using the AnadigmDesigner2 software for an AN231E04 FPAA device. Two signal paths allow different clock rates for the anti-alias (upper) and one-third octave (lower) filters.

Clocks, noise and aliasing

The clock structure within the AN23x series of FPAAs provides three clock types: a master clock, two system clocks and six analogue clocks. Both system clocks derive from the master clock using individual clock dividers (even integers up to 510). System clocks are then divided to give the analogue clocks. The analogue clocks are assigned to the signal chains (although a clock divider of unity is available so the master clock can be passed through to an analogue clock if required). All elements in a signal chain, that is all CAB elements joined between an input IOCell and an output IOCell, are forced to use the same analogue clock.

For a given signal chain the dominant clock noise was observed at the analogue clock frequency (the analogue clock chosen to drive the signal chain). Surrounding the analogue clock noise was an additional alias signal, introduced through modulation of the input signal by the analogue clock. To reduce the aliasing effect two signal chains were constructed, each having a different analogue clock. The first signal chain contained a variable frequency anti-alias filter with an analogue clock frequency considerably higher than the cut-off frequency of the filter. The second signal chain contained the two sub-filters and a gain stage for the one-third octave filter. The second signal chain was clocked at a frequency much lower than the frequency of the clock used in the first anti-alias filter stage. The two stage filtering arrangement significantly reduced the aliasing effect.

Another form of interference was discovered when sweeping through the bank of one-third octave filters. During the sweeping operation a number of different analogue clock selections were required to keep the filter frequency to clock frequency ratios within defined limits. When a clock selection was changed an additional signal was observed in the output requiring additional settling time.

Programming and controlling the FPAA

Control of the FPAA device was achieved using a microcontroller programmed with the ability to pre-compute individual filter parameters and timing requirements for each stage in the sweeping process. When operating in sweeping mode the microcontroller computed indexing into the pre-computed lookup tables for the filter parameters and then mapped these values to a re-configuration buffer. A short period of time was required to transmit the re-configuration buffer from the microcontroller to the FPAA device over an SPI bus. Following re-configuration a settling time was enforced to allow the effects of clock and switching changes to reduce to acceptable levels. The required settling time was at least the inverse of the bandwidth of the filter set during the re-configuration; however it was found that in practice a longer amount of time was required. A settling time of ten times the inverse of the bandwidth of the filter was chosen for the sensor.

To allow post processing analysis of the sensor, as previously discussed, a timing channel was output from the microcontroller to differentiate between periods of valid and invalid data from the FPAA. The timing channel was produced by switching a single pin on the microcontroller. A low value was used for invalid periods, such as when re-programming the FPAA or waiting for a configuration change to settle, and a high value used when the output of the FPAA was considered valid. The only disadvantage of this approach was that the timing signal from the microcontroller required DC coupling with the recording device, which precluded the use of many simple audio recording devices. To ensure accurate recording of the timing channel a DC-coupled Data Translation DT9636 ADC was used to simultaneously capture the timing signal, sensor output and raw input signals.

Exposure times

Exposure time was a term used to describe the total length of time of valid data from the FPAA used for each one-third octave band level estimate. The choice of exposure time affects the variability of the one-third octave estimate (Blackman & Tukey 1958) and can be guided by a desired estimation uncertainty. The expected spread of mean square estimates ($\hat{s}$) in decibels can be expressed as a function of the exposure time (Δt) in seconds for each one-third octave band and filter bandwidth (BW) in Hz as shown in Equation 4 (see for example Dirac Delta Consultants Ltd. 2009).

$$\hat{s} = \frac{4.34}{\sqrt{(\Delta t \times BW) - \frac{1}{2}}} \tag{4}$$

For a desired estimation uncertainty no greater than $2\hat{s}$ and for convenience assuming $(\Delta t \times BW) + ½ \approx (\Delta t \times BW)$, the exposure time Δt in seconds can be chosen using Equation 5. The reason for obtaining a simple expression for Δt was to minimise computation required within the microcontroller. Note that the expression on the right hand side of Equation 5 contains the desired spread of noise power $\hat{s}$ in dB and the filter bandwidth BW in Hz, and is a minimum choice for the exposure time.

$$\Delta t \geq \frac{18.8}{\hat{s}^2 BW} \tag{5}$$

Given a choice of Δt the actual spread of uncertainty in the one-third octave estimate must be computed by re-substituting the choice of Δt back into Equation 4. In practice the overall estimation uncertainty will be slightly higher than the value computed using Equation 4 due to ripple in the passband of each filter. For a Type-3 ANSI filter the allowable passband ripple is 200 millibels (ANSI S1.11-1986).

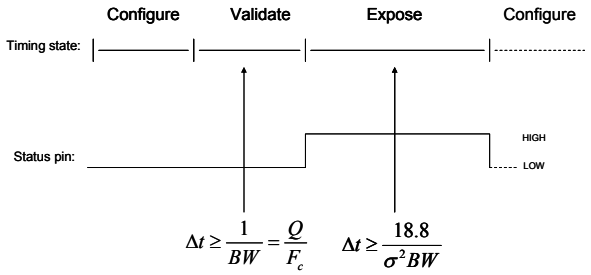

Figure 2. Timing control of the FPAA allowing for configuration and validation of each new filter before exposing the filter for estimation of the one-third octave level. The value F_c is equal to the value f_c used in the text.

Implementing the exposure times in the microcontroller required pre-computing values for each filter and compiling a lookup table. Upon successful dynamic configuration of the FPAA the timing channel pin was set high (as discussed previously), the required exposure time was taken from the lookup table and passed to an interval control routine in the microcontroller.

RESULTS

Laboratory testing

Laboratory testing included filter characterisation using a network analyser and sensor testing using white noise and pink noise from a signal generator.

Filter characterisation was conducted using an Agilent 4395A analyser. The analyser was configured as a network analyser using a signal power of 0 dBm (into 50Ω) on the output and Agilent 41802A input adapters on inputs R (reference) and B (device-under-test) to raise the input impedance to 1MΩ. In this mode the reference 1 kHz filter response was measured and is shown in Figure 3. The passband gain response of the filter set was measured to give a set of gain corrections for an overall unity gain and the corrected full response of every filter in the bank was measured (shown in Figure 5).

Figure 3 shows the measured response of the reference 1 kHz one-third octave filter (solid line) and the allowable limits according to the ANSI Order-2 Type 3-D standard. The response of the realised filter lies at the centre of the limits indicating good agreement with the standard in the filter skirts.

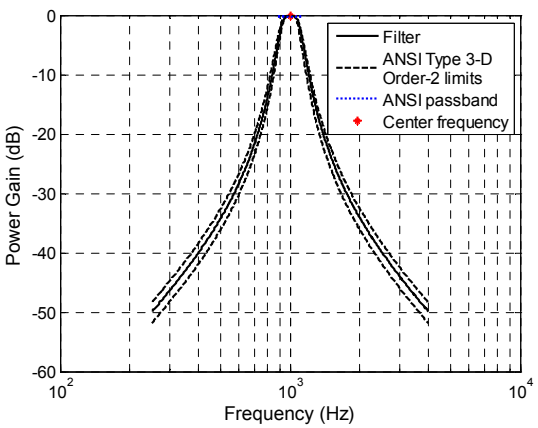

Figure 3. The reference 1 kHz filter gain (solid line) lies within the bounds for an Order-2 ANSI Type 3-D filter (dashed lines).

A zoom to the passband of the reference filter (solid line) is shown in Figure 4. The exact design centre frequency of the filter is shown and the ANSI limits are symmetric about that frequency. It is evident that the realised filter's centre frequency is slightly higher than the design frequency, due to accuracy limitations imposed on the two sub-filters by the choice of analogue clocking frequency. Asymmetry in the position of the realised filter response within the ANSI limits is due to the offset centre frequency. Also shown in Figure 4 is an estimate of the region where variation in the filter response through the passband may not be ideal (horizontal dotted lines). The choice of legend text *ANSI passband* for this region indicates variation to compare with the ANSI standard; it does not indicate the allowable ANSI limits (which may be much larger). Variation of the measured filter passband response was within the maximum allowable limit for an ANSI Type-3 filter.

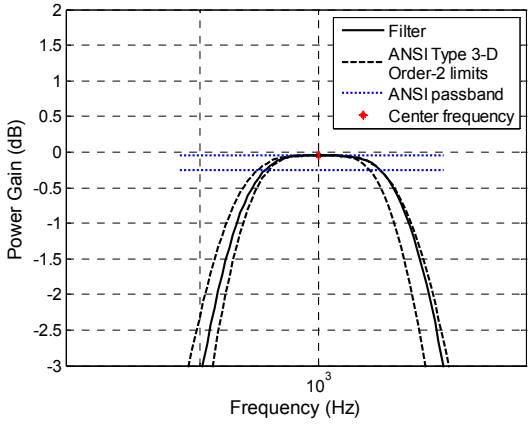

Figure 4. Passband of the 1 kHz reference filter (solid line) showing an estimate of the region where variation in the filter response through the passband may not be ideal (horizontal dotted lines).

Characterising of the filter bank was achieved by measuring the response of every individual filter in the filter bank using the measurement process outlined for the reference filter. During the measurement process the Intermediate Frequency (IF) bandwidth was varied to give a reasonable compromise between measurement accuracy and speed. An IF bandwidth of 10 Hz was used when measuring the filters from ANSI bands 20 and 24, a 30 Hz IF bandwidth for bands 25 to 32 and a 100 Hz IF bandwidth for bands 33 and above. Results are shown in Figure 5.

Symmetry between the filters shown in Figure 5 provides an indication of uniformity of filter characteristics across the filter bank. The passband maximum values approach within 0.1 dB of unity gain (0 dB) for each filter and the transitions between filters lie within the -3 dB zone. The skirts of each filter attenuate at approximately 12 dB per octave (40 dB per decade) consistent with a Butterworth filter of order two. The effect of anti-alias filtering can be seen in the tails of the filter skirts, particularly at the high frequency end of the filter bank. A slight tilt through the passband of the 20 kHz filter can also be seen and is attributed to the same cause.

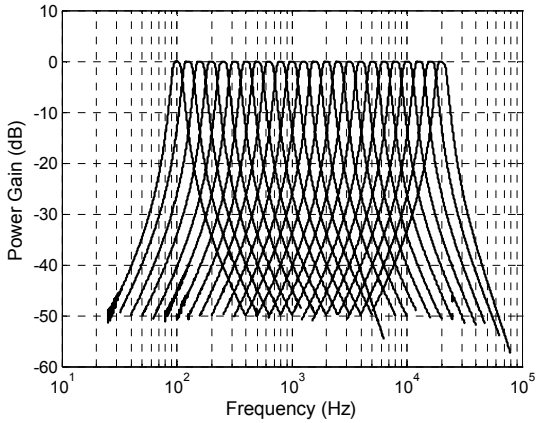

Figure 5. Characteristic curves for all 23 filters in the one-third octave filter bank. Gain corrections have been applied to give a unity (0 dB) response for each filter. The slight skew at high frequencies is due to anti-alias filtering.

Sensor operation in sweeping mode was bench tested using white noise and pink noise. A Neutrik Minirator MR1 audio signal generator was used to generate the white and pink noise. Output from the MR1 was split and fed into both the one-third octave sensor and one of the inputs of a Data Translation DT9836 USB data acquisition module. The two outputs from the one-third octave sensor were also fed into the DT9836. All three signals entering the DT9836 were simultaneously sampled at a sample rate of 100 kHz and the data stored on a laptop for post-processing. Exposure times were chosen to give a fixed time-bandwidth product ($\Delta t \times BW$) of 6.3. Post-processing comprised of a MATLAB code to detect valid data regions using the status pin data, extract valid sections of filtered data, concatenate the valid data and compute a RMS estimate. Adjustments were applied to the RMS estimates for displaying on a power spectral density plot.

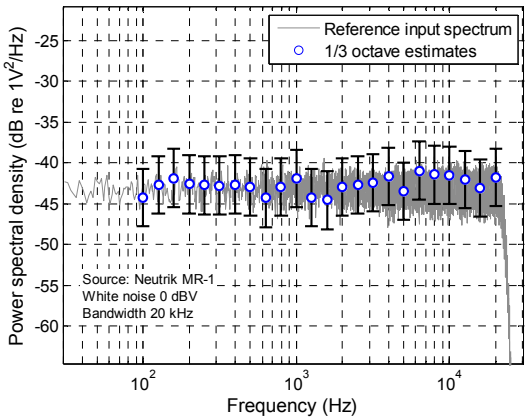

Figure 6. Comparison of white noise input spectrum with one-third octave sensor response to a 0 dBV white noise input spectrum with 20 kHz bandwidth.

Figure 6 shows a comparison of sensor estimates (circle markers with error bars) with a Welch power spectral density curve (dark grey line) for 0 dBV white noise bandwidth limited to 20 kHz. The sensor one-third octave estimates agree with the input signal within an uncertainty ($\pm 2\hat{s}$) of ±3.53 dB; however the variability in sensor estimates were greater than expected. Inspection of the filter output using a spectrogram showed the expected clock noise and aliasing features interfering at frequencies higher than the centre frequency of the filter. What was also noticed was interference at the centre frequency of the filter following a transition of the analogue clock. This clock transition interference was reduced by extending the amount of time waiting in the validation state (prior to exposure) but not eliminated entirely.

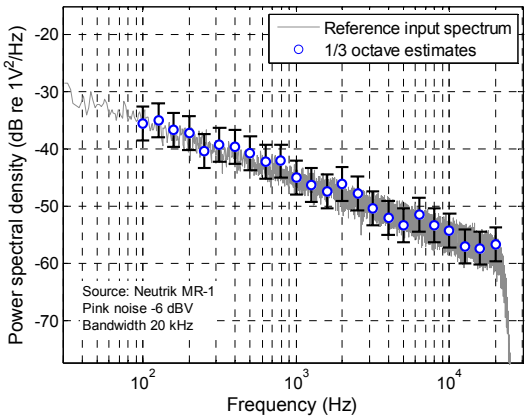

Figure 7. One-third octave power estimates produced by the sensor converted to spectral densities (circles with error bars) plotted against the power spectral density of a -6 dBV over 20 kHz reference pink noise input signal (dark grey line).

Figure 7 shows a similar plot for a -6 dBV pink noise input signal bandlimited to 20 kHz. The sensor estimates agree with the input spectrum within uncertainty but variability in the estimates is increased by the clock noise, aliasing and clock transition interference.

Field measurements

A set of field measurements were taken in Cockburn Sound to prove the operation of the sensor in its intended application. An HTI-96-MIN hydrophone was suspended from a set of pontoons at a depth of 5 m. The hydrophone output was passed through a Stanford Research SR560LN preamplifier and filter to allow additional matching of the hydrophone output to the one-third octave sensor input. A Data Translation DT9636 USB data acquisition module was used to capture the three information signals output from the sensor and the results were recorded on a laptop. This configuration was used to allow flexibility of the input to the sensor while maintaining the same sensor structure, configuration parameters and post-processing that was used for bench testing. Results from the measurement are shown in Figure 8 using the same layout as was used for the white and pink noise tests.

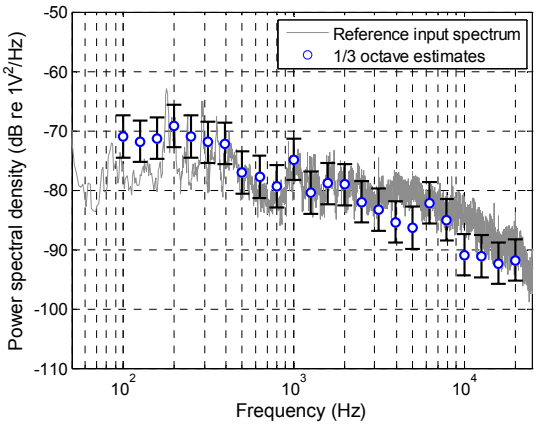

Figure 8. Results of field measurements conducted in Cockburn Sound.

DISCUSSION

Mathematical filter design equations given in (Kugelstadt 2002) were sufficient to provide the required sub-filter parameters for implementing a one-third octave filter in an FPAA. A numerical solution was required for parameter α and the MATLAB *solve* routine was able to provide a suitable solution. When cascading the two sub-filters the desired filter response was realised in a single FPAA device. Measurement of the reference 1 kHz filter agreed with the ANSI standard for an Order-2 Type 3-D one-third octave filter. A terminology difference between the mathematical order of the filter used in the design process and the order specified in the ANSI standard was identified and caused some initial concern; however a check of the skirt attenuation as a function of frequency confirmed it as a terminology difference only.

Laboratory measurement of the filter bank characteristics (static response) and bench testing of sensor operation in sweep mode (dynamic response) were expected to be consistent, that is, the filter characteristics were expected to give an indication of dynamic sensor operating performance. In practice the dynamic response was more variable. Factors contributing to the increased variability of dynamic results include: additional filtering in the network analyser when measuring the filter characteristics (improving the static results), and the relatively short settling time between analogue clock transitions and measurement during sensor sweep operation (degrading the dynamic results). Despite the increased variability during dynamic operation the sensor estimates were within an acceptable uncertainty for both white and pink noise. Field tests in Cockburn Sound confirmed the sensor operation in a real environment.

CONCLUSION

A dynamic configurable sensor for fractional-octave-band underwater measurement has been designed, implemented, tested in the laboratory and proven in the field. It is concluded that a single FPAA device can be used for the sensor and that the demonstration sensor has achieved the intended objective. Work is underway to produce a small self-contained version of the sensor to be used in the field.

REFERENCES

American National Standards Institute 1986, *Specification for Octave-Band and Fractional-Octave-Band Analog and Digital Filters*, ANSI S1.11-1986, American National Standards Institute, Washington, DC

Anadigm Company 2008, 'AN231E04 Datasheet Rev 1.1: 3rd Generation Dynamically Reconfigurable dpASP', Online manual, viewed 11 May 2009, <http://www.anadigm.com/_doc/DS231000-U001.pdf>

Antoni, J 2010, 'Orthogonal-like fractional-octave-band filters', *J. Acoust. Soc. Am.* vol. 127 no. 2 pp. 884-895

Baccigalupi, A & Liccardo, A 2007, 'Field programmable analog arrays for conditioning ultrasonic sensors', *IEEE Sensors Journal,* vol. 7 no. 8 pp. 1176-1182.

Becker, J, Henrici, F, Trendelenburg, S & Manoli, Y 2008, 'A rapid prototyping environment for high-speed reconfigurable analog signal processing', in *Proceedings of the 22nd IEEE International Parallel and Distributed Processing Symposium, IPDPS 2008*, Miami, FL

Bjor, O 2008, 'Filters', in D Havelock, S Kuwano & M Vorländer (eds.), *Handbook of Signal Processing in Acoustics*, Springer, New York, NY

Blackman, RB & Tukey, JW 1958, *The measurement of power spectra from the point of view of communications engineering*, Dover Publications Inc., New York

Dahl, PH, Miller, JH, Cato, DH & Andrew, RK 2007, 'Underwater ambient noise', *Acoustics Today* vol. 3 no. 1 pp. 23-33

Dirac Delta Consultants Ltd. 2009, *Science & Engineering Encyclopedia – Version 2.3,* Online resource, viewed 14 July 2009, < http://www.diracdelta.co.uk/science/source/o/c/octave/source.html>

Eriksen, CC, Osse, TJ, Light, RD, Wen, T, Lehman, TW, Sabin, PL, Ballard, JW & Chiodi, AM 2001, 'Seaglider: A long-range autonomous underwater vehicle for oceanographic research', *IEEE J. Oceanic Eng.* vol. 26 no. 4 pp. 424-436

Hall, TS, Twigg, CM, Gray, JD, Hasler, P & Anderson, DV 2005, 'Large-scale Field-Programmable Analog Arrays for analog signal processing', *IEEE T. Circuits-I*, vol. 52 no. 11 pp. 2298-2307

Koay, TB, Tan, YT, Eng, YH, Gao, R, Chitre, M, Chew, JL, Chandhavarkar, N, Khan, RR, Taher, T & Koh, J 2010, 'STARFISH – A small team of autonomous robotic fish', in *3rd International Conference on Underwater System Technology: Theory and Applications 2010*, Cyberjaya, Malaysia

Kouider, M, Nadi, M, Kourtiche, D, Prado-Olivarez, J & Rouane, A 2003, 'Hardware and software implementation for an auto-calibrated measurement system', in *Proceedings of IEEE Sensors*, vol. 2 no. 1, pp. 611-616

Kugelstadt, T 2002, 'Active filter design techniques', in R Mancini (ed.), *Opamps for everyone – design reference*, Texas Instruments Inc., Dallas, Texas, viewed 21 February 2011, <http://focus.ti.com/lit/an /slod006b/slod006b.pdf>

Lavoie, P & Pollard, A 2001, 'Analysis of four data reduction schemes applied to four-sensor hot-wire probes', in *Proceedings of the 14th Australiasian Fluid Mechanics Conference*, Adelaide University, Adelaide Australia

Matthews, D, MacLeod, R & McCauley, RD 2004, 'Bio-Duck activity in the Perth Canyon: An automatic detection algorithm', in *Proceedings of ACOUSTICS 2004*, Gold Coast, Australia, pp. 63-66

Merendino, G, Callegari, S, Golgarelli, A, Zagnoni, M & Tartagni, M 2005, 'Signal conditioning for capacitive sensors with Field Programmable Analog Arrays', in *Proceedings - ISSCS 2005: International Symposium on Signals, Circuits and Systems*, Lasi, Romania, pp. 139-142

Morales, DP, Garcia, A, Castello, E, Carvajal, MA, Banqueri, J & Palma, AJ 2010, 'Flexible ECG acquisition system based on analog and digital reconfigurable devices', *Sens. Actuators A: Phys.,* doi:10.1016/j.sna.2010.10.008

Morales, DP, Garcia, A, Palma, AJ, Carvajal, MA, Castillo, E & Capitán-Vallvey, LF 2008, 'Enhancing ADC resolution through Field Programmable Analog Array dynamic reconfiguration', in *Proceedings - 2008 International Conference on Field Programmable Logic and Applications, FPL 2008*, Heidelberg, Germany, pp. 635-638

Simão, N, Escartín, J, Goslin, J, Haxel, J, Cannat, M & Dziak, R 2010, 'Regional seismicity of the Mid-Atlantic Ridge: observations from autonomous hydrophone arrays', *Geophys. J. Int.* vol. 183, pp 1559-1578

Smith, JO 2008 (Draft), 'Spectral Audio Signal Processing', Online book, viewed 24 May 2011. <http://ccrma.stanford.edu/~jos/sasp/>